Shift-Invariant Motif Discovery in Image Processing

Sahar Torkamani and Volker Lohweg, Senior Member, IEEE
inIT – Institute Industrial IT
Ostwestfalen-Lippe University of Applied Sciences
Lemgo, Germany
Email: {sahar.torkamani, volker.lohweg}@hs-owl.de

***Abstract*—Nowadays, the boost of optical imaging technologies results in more data with a faster rate are being collected. Consequently, data and knowledge discovery science has become an attractive and a fast growing topic in several industry and research area. Motif discovery in image processing aims to tackle the problem of deriving structures or detecting regularities in image databases. Most of the motif discovery methods first convert images into time series and then attempt to find motifs in such data. This might lead to information loss and also the problem of inability to detect shifted and multi-scale image motifs of different size. Here, a method is proposed to find image motifs of different size in image datasets by applying images in original dimension without converting them to time series. Images are inspected by the Complex Quad Tree Wavelet Packet transform which provides broad frequency analysis of an image in various scales. Next, features are extracted from the wavelet coefficients. Finally, image motifs are detected by measuring the similarity of the features. The performance of the proposed method is demonstrated on a dataset with images from diverse applications, such as hand gesture, text recognition, leaf and plant identification, etc.**

Keywords–Motif discovery; Image processing; Wavelet transformation.

I. INTRODUCTION

In this new millennium, the growth of digital computation and telecommunication has resulted in a flood of information. Most of this information is in the form of text, graphics, pictures, videos or integrated multimedia. In order to analyse and acquire efficient information from such datasets, data mining and machine learning tasks are essential. These tasks can be categorized into clustering, classification, anomaly detection and *motif discovery*.

In order to perform the aforementioned tasks, one needs to have information such as number of clusters or classes, prototype patterns/images for each class and a given image query to find [1]. The problems of clustering or classifying images as well as finding the query images in an image database have been investigated during last decades [2]–[4]. However, the problem of deriving structures or detecting regularities in image databases is rather new topic and investigated by researchers [5]. Detecting frequently repeated unknown images in a data base without any prior information is called motif discovery. The term motif finds its origin in genetics and Deoxyribonucleic Acid (DNA) sequence. A sequence motif in a DNA is a widespread amino-acid sequence pattern which shows a biological significance [6]. However, this term was first triggered by Patel et al. [7] in time series data mining.

Motifs provide valuable insights about the investigated problem to the user. In the past decade, huge research effort has been performed on this topic [5] [8]. However, most of the image motif discovery methods, first convert images into one-dimensional time series and then attempt to find motifs in such data. This might leads to information loss and also the problem of inability to detect shifted and multi-scale motifs of different size [9]. Correspondingly, a method is proposed to find shifted and multi-scale motifs of different size in image datasets by applying the images in original dimension without converting them to one dimensional time series.

The paper is structured as follows: the related work in motif discovery for image data type is described in Section II. The proposed approach is explained in Section III. Next, evaluation of this method and the obtained results are illustrated in Section IV. Finally, the directions of the future work and a conclusion are indicated in Section V.

II. RELATED WORK

Image and shape analysis have been a matter for discussion over the past decades. Huge amount of research has been performed in several image processing tasks such as clustering, classification, query by content, segmentation, etc. [3], [10]–[13]. Recently, motif discovery in image and shape analysis has gained great interest. Researchers aimed to link time series data mining tasks and issues to the image and shape analysis domain [5] [9] [14].

First, Xi et al. [9] tried to detect image motifs in image data sets. Nevertheless, their approach is based on representing an image or a shape in a one dimensional time series. The main problem of such an approach is that transforming a two dimensional data to a one dimensional might lead to information loss.

Chi et al. [15] applied the same procedure as in [9] in order to detect image motifs in face image data sets. Ye and Keogh [14], as well as Grabocka et al. [16] extended the proposed approach in [9] by introducing the term shaplet. After transforming an image to a one dimensional representation, instead of analysing the whole time series only a discriminative subsequence of the time series will be considered. Although the performance of these methods is promising, but these approaches transform the data to a one dimensional time series.

Recently, Rakthanmanon and his colleagues [17] aimed to tackle this problem by detecting motifs in image data without representing them into a one dimensional signal. In [17], first images are segmented using a sliding window of a fixed size, then the similarity between these segments are measured by the generalized Hough transform. One of the drawback of this method is the size of the window. This results in inability of detecting motifs with various proportions. En et al.

 ISBN: 978-1-61208-549-4

[18] followed a similar approach, nevertheless they employed sliding windows with varying sizes of 20, 40, 80, 160 pixels.

In our previous approach [19] motifs in an image data base are discovered in their original dimension without converting them to time series. Images are decomposed into several frequency scales by the dual tree complex wavelet transform (DTCWT) [20], next features are extracted from the wavelet coefficients and finally motif images are found by measuring the similarity of their features. However, further experiments showed that the DTCWT is shift tolerance and not shift invariant [21]. For this reason, in this work, an approach is proposed which is based on a shift-invariant feature extraction method for motif discovery (SIMD), given in [21]. This method is applied as core in our approach and explained in the following section.

III. Proposed Approach

The sketch of our approach is depicted in Figure 1.

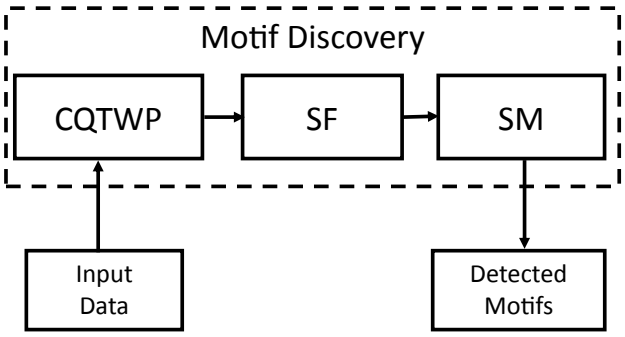

Figure 1. The proposed approach; CQTWP is the Complex Quad Tree Wavelet Packet; SF are the statistical features and SM are similarity measures.

In the first step, images are transformed by the *Complex Quad Tree Wavelet Packet* (CQTWP) into a broad frequency scales. After that features are extracted from the normalized wavelet coefficients. Finally, motifs are discovered by measuring the similarity between features using various distance measures. These steps are explained in details in the following.

A. Complex Quad Tree Wavelet Packet Transform

1) 1D-CQTWP: The CQTWP is an extended version of the DTCWT [20] and it consists of two wavelet packet trees working parallel to each other; namely "WPT A" and "WPT B" where "WPT A" represents the real part and "WPT B" provides the imaginary part of the signal. Figure 2 is a graphical representation of the "*1D-WPT A*", where $\downarrow 2^e$ and $\downarrow 2^o$ depict the even and odd down-sampling.

The wavelet and scaling functions of the CQTWP are defined as:

Definition 1. *Let* $\psi_{a,2J+1}(t)$,$\psi_{a,2J+3}(t)$, $\psi_{b,2J+1}(t)$, $\psi_{b,2J+3}(t)$ *and* $\phi_{a,2J}(t)$,$\phi_{a,2J+2}(t)$, $\phi_{b,2J}(t)$, $\phi_{b,2J+2}(t)$ *be the wavelet and scaling functions of the CQTWP. For convenience both wavelet transforms are considered as orthonormal. The wavelet and scaling functions in "WPT A",*

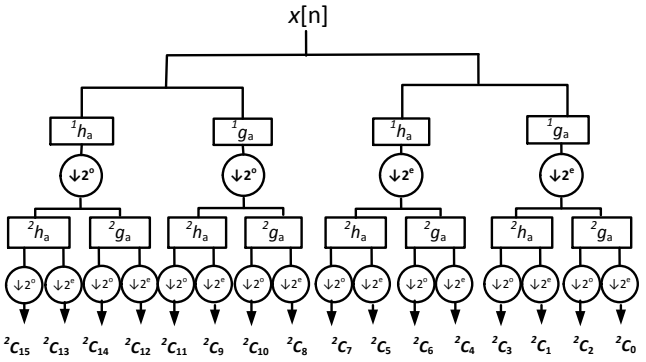

Figure 2. First wavelet packet filter bank of a two scale CQTWP. The filters $^s g_a$ and $^s h_a$ are low and high pass filters and s is the number of scales.

$\forall n \in \mathbb{N}$ *are given by*

$$^{s+1}\psi_{a,2J+1}(t) = \sqrt{2}\sum_{n=0}^{M} {}^s h_a[n]\ {}^s\phi_{a,2J}(2t-n),$$

$$^{s+1}\psi_{a,2J+3}(t) = \sqrt{2}\sum_{n=0}^{M} {}^s h_a[n]\ {}^s\phi_{a,2J+2}(2t-n+1),$$

$$^{s+1}\phi_{a,2J}(t) = \sqrt{2}\sum_{n=0}^{M} {}^s g_a[n]\ {}^s\phi_{a,2J}(2t-n),$$

$$^{s+1}\phi_{a,2J+2}(t) = \sqrt{2}\sum_{n=0}^{M} {}^s g_a[n]\ {}^s\phi_{a,2J+2}(2t-n+1).$$

Parameter $J = 2j$ *where* $0 \leq j < 2^s \cdot (s-1)$*, and* $s \in \mathbb{N}$ *is number of scales.*

For "WPT B" the wavelet and scaling functions are defined in the same manner, but the high-pass filter $^s h_a$ *and the low-pass filter* $^s g_a$ *are replaced by* $^s h_b$ *and* $^s g_b$ *respectively. All filters are causal so* $^s h_{a,b}[n] = 0$ *and* $^s g_{b,b}[n] = 0$ *for* $n < 0$*.*

The CQTWP applies the same filters as the DTCWT whereby the filters are real and orthonormal. In the first scale, the filters have the even-length of 10 [22] and in the scale greater than one, filters have the even-length of 14. Both filters form a Hilbert pair due to their design [20].

Definition 2. *Wavelets* ψ_a *and* ψ_b *with the following property*

$$\Psi_a(j\omega) = \begin{cases} -j\Psi_b(j\omega), & \omega > 0, \\ j\Psi_b(j\omega), & \omega < 0, \end{cases}$$

are called the Hilbert pair*, where* $\Psi(j\omega)$ *is the Fourier transform of* $\psi(t)$*.*

This means, the response of each branch of the "WPT A" and the corresponding branch of the "WPT B" forms a Hilbert pair. Consequently, the CQTWP is approximately analytic in each sub band. The analytic representation has advantages such as reduction of aliasing.

The CQTWP has another advantage of being shift-invariant [21]. This property is achieved by decomposing a non shifted and a shifted version of the input signal in each scale. Shift-invariance property results in identical wavelet coefficients for

both the original signal and its shifted versions. In other words, the wavelet and scaling functions of the CQTWP select both even and odd samples of the signal in order to detect the occurred shift. For simplicity, the wavelet and scaling functions of "WPT A" are denoted by $\psi_{a,e}(t) = \psi_{a,2J+1}(t)$ and $\psi_{a,o} = \psi_{a,2J+3}(t)$; and $\phi_{a,e} = \phi_{a,2J}(t)$, $\phi_{a,o} = \phi_{a,2J+2}(t)$. The functions of "WPT B" are represented in the same manner. The proof of shift invariance property of the CQTWP is given in [21].

2) 2D-CQTWP: The first scale of the 2D-CQTWP is similar to the 2D-discrete wavelet transform [23], where an image is decomposed into four sub bands namely LL_1, LH_1, HL_1 and HH_1, cf. Figure 3(a). However, in the first scale the 2D-CQTWP has two LL, two LH, two HL and two HH sub bands obtained from both "*2D-WPT A*" and "*2D-WPT B*".

The structure of two scales decomposition of the "*2D-WPT A*" is depicted in Figure 3(b) where both low and high-pass filtered sub bands decomposed further. This property results in a more flexible and broad frequency decomposition of the images.

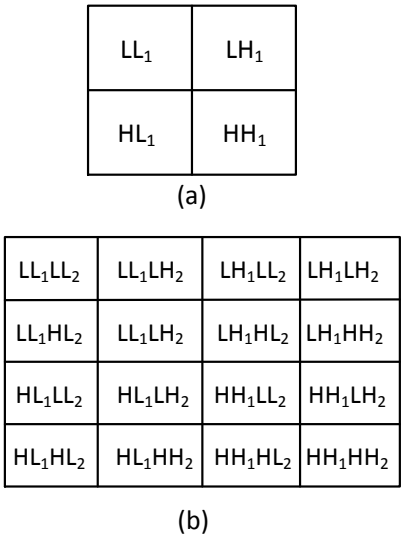

Figure 3. Structure of two scales decomposition of the "*2D-WPT A*": (a) the first scale decomposition, (b) the second scale decomposition.

LL_1 is the product of the low-pass function $\phi_a()$ along the first dimension (row) and the low-pass function $\phi_a()$ along the second dimension (column). LH_1 is the product of the low-pass function $\phi_a()$ along the first dimension (row) and the high-pass function $\psi_a()$ along the second dimension (column). Similarly the HL_1 and HH_1 are labelled, and the index 1 determines the decomposed scale. The same procedure is performed on each subband in order to obtain the second scale coefficients.

The wavelet and scaling functions of the 2D-CQTWP are defined as:

Definition 3. *The "2D-WPT A"of the 2D-CQTWP is characterized by twelve wavelets and four scaling functions. The 2D-wavelet $\psi(x,y) = \psi(x)\psi(y)$ is associated with the row-column implementation of the wavelet transform. The wavelet functions for the wavelet packet tree A are given by*

$$\psi_{a,1}(x,y) = \phi_{a,e}(x)\psi_{a,e}(y), \qquad \psi_{a,4}(x,y) = \phi_{a,e}(x)\psi_{a,o}(y),$$
$$\psi_{a,2}(x,y) = \psi_{a,e}(x)\phi_{a,e}(y), \qquad \psi_{a,5}(x,y) = \psi_{a,e}(x)\phi_{a,o}(y),$$
$$\psi_{a,3}(x,y) = \psi_{a,e}(x)\psi_{a,e}(y), \qquad \psi_{a,6}(x,y) = \psi_{a,e}(x)\psi_{a,o}(y).$$

The rest of the wavelet functions are obtained similarly. The scaling functions are defined as

$$\phi_{a,1}(x,y) = \phi_{a,e}(x)\phi_{a,e}(y), \qquad \phi_{a,2}(x,y) = \phi_{a,e}(x)\phi_{a,o}(y),$$
$$\phi_{a,3}(x,y) = \phi_{a,o}(x)\phi_{a,e}(y), \qquad \phi_{a,4}(x,y) = \phi_{a,o}(x)\phi_{a,o}(y).$$

The wavelet and scaling functions of the "2D-WPT B" are given accordingly.

B. Feature Extraction

Features present the special characters of the data, therefore it is important that they are detectable under changes in proportion, location or even under noise circumstances. Before extracting features, coefficients of each scale must be normalized by a normalized histogram. The normalized histogram $H(p)$ is given by

$$H(p) = \frac{1}{v \cdot u} \cdot h(p),$$

where $u, v \in \mathbb{N}$ determine the size of the matrix coefficients and parameter p is number of the histogram bins. The rate in each bin is presented by $h(p)$.

The extracted features are the first four statistical moments [24], namely, mean value, variance, skewness and kurtosis which are derived from the wavelet coefficients in both wavelet packet trees. As CQTWP is shift-invariant, then these features have identical values even in the case of shift occurrence in the data.

The scaling and wavelet functions of the CQTWP are orthonormal, and according to the Parseval's theorem the energy of the signal (image) is preserved in the coefficients. Therefore, the energy of the wavelet coefficients and their shifted ones are similar. As a result, in addition to statistical features, energy of the wavelet coefficients is considered as another feature.

C. Similarity Measures

In order to detect image motifs, the similarity between their features must be measured. Most cited and applied distance similarity measures in motif discovery are: two members of the Minkowski distance family [25], and Dynamic Time Warping (DTW) [25], which are applied as well in this work. The two members of the Minkowski distance or L_p-distance, Euclidean distance (ED) and Canberra distance (CD), both have linear computational time complexity $O(n)$, and are metric.

The Euclidean distance is obtained by setting $p = 2$ in L_p-distance. This measure is also known as L_2-distance. Besides the advantages of the Euclidean distance, results of this similarity measure are not promising in the case of outliers. The Canberra distance is actually a weighted version of Manhattan distance or L_1-distance, and is useful in the case of ranking lists or results.

DTW matches various sections of a time series by warping of the time axis, or finding the proper alignment. This similarity measure is more flexible than Euclidean or Canberra distance although its time-complexity is $O(n^2)$. Besides its quadratic computational time complexity, still DTW is one of the most popular approaches for measuring similarity/dissimilarity.

 ISBN: 978-1-61208-549-4

IV. Experiments and Results

To evaluate the performance of the proposed approach, the results are analysed by different quality measures, explained in the following. Next, the captured results of image motif discovery are presented.

A. Quality Measures

A perfect image motif is the one which matches all the images in the target class and no other images out of that class. To evaluate the result following quality measures are employed [1]: Correct motif discovery rate CR, Sensitivity Sn, Precision Pr and F-Measure $F-M$. These quality measures are based on four possibilities to qualify a motif matching an image; namely, true positive rate (TP), false negative rate (FN), true negative rate (TN), and false positive rate (FP).

Correct motif discovery rate is given by $CR = \frac{n^+}{N}$ where N is number of all motifs and n^+ is number of correctly detected motifs. Sensitivity ($Sn = \frac{TP}{TP+FN}$) measures the capacity of images of the target class correctly matched by the motif, Precision ($Pr = \frac{TP}{TP+FP}$) provides the fraction of images of the target class that are matched by the motif and the images that are not correctly matched by the motif and finally both precision and sensitivity are considered by F-Measure ($F-M = 2 \cdot (\frac{Pr \cdot Sn}{Pr+Sn})$) [1].

B. Results and Evaluation

The test image data base consists of images from diverse applications and domains like hand gesture and leaf identification [26], [27]. All the tests are executed with a 3.40 GHz Intel(R) core processor with 8GB RAM. The codes are performed by MATLAB R2015b [28]. In Figure 4, images of four groups are depicted. These images have various size and scale, since the proposed method is able to handle both images of fixed and variable size.

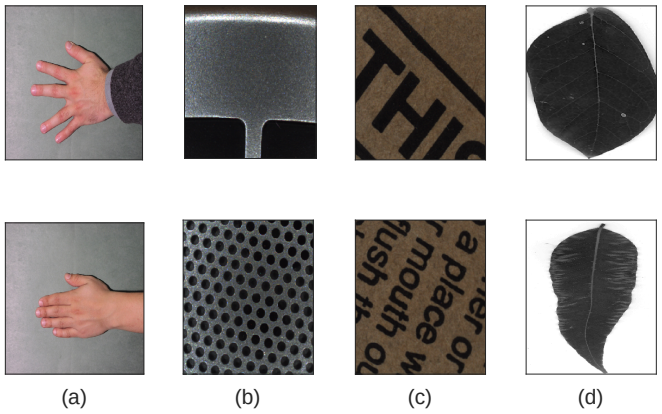

Figure 4. Data set of different images.

Among these images, the pictures of hands and leaves are the most occurred images (top inserted image motifs). Figure 5 shows the inserted image motifs (hand and leaf). In order to demonstrate the shift-invariant property of the 2D-CQTWP in feature space, images (b-d) are considered. These images are the shifted version of the image (a), and image (e) is the rotated version of image (a). Images (f-j) are different leaf types.

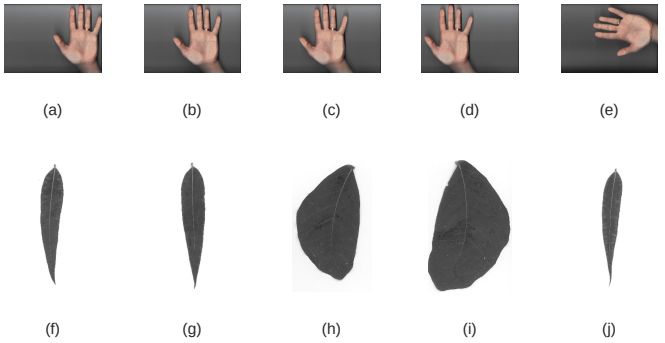

Figure 5. Images of hands and leaves. Images (b-d) are the shifted version of image (a); Image (e) is the rotated version of image (a). Images (f-j) are various sorts of leaves.

In the preprocessing step, all the images are presented in grey-scale, since the colour information is not required. Next, all the images are sent to 2D-CQTWP and decomposed into various scales. In this work, the wavelet coefficients of the second scale are selected, since the amount of noise is usually reduced in the second scale for the noisy data. The normalized histogram of the wavelet coefficients are calculated. Figure 6 is the graphical representation of the normalized histogram of the HL sub band coefficients of "2D-WPT A".

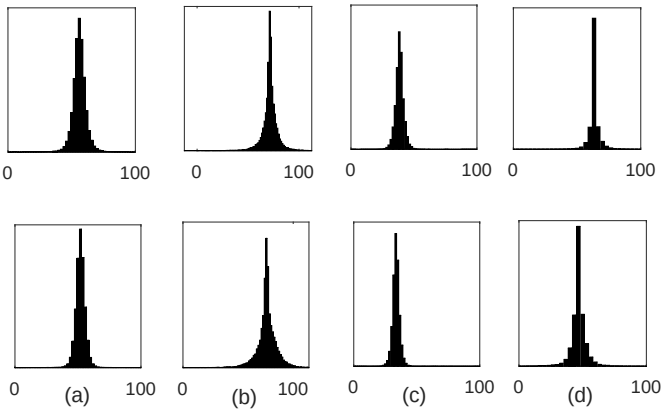

Figure 6. Normalized histogram of the HL sub band coefficients, obtained from the corresponding images from Figure 4 (a-d).

As depicted, the histograms of wavelet coefficients from the two depicted images in each group (a), (b), (c) and (d) are similar to each other but different to the histograms of other groups. This helps to determine the variations between various motif classes (inter-class).

The shift-invariant property of the 2D-CQTWP can be observed in Figure 7. A hand pattern and its shifted version is depicted in Figure 7 (a)-(b), where the position of the hand is changed. The normalized histogram of the HL sub band coefficients are given in Figure 7 (c)-(d) respectively. Since the 2D-CQTWP is shift-invariant, the histograms are identical to each other.

Next, the five stated features are extracted from the histograms of the wavelet coefficients in each scale. The efficiency of these features are tested by the linear discriminant

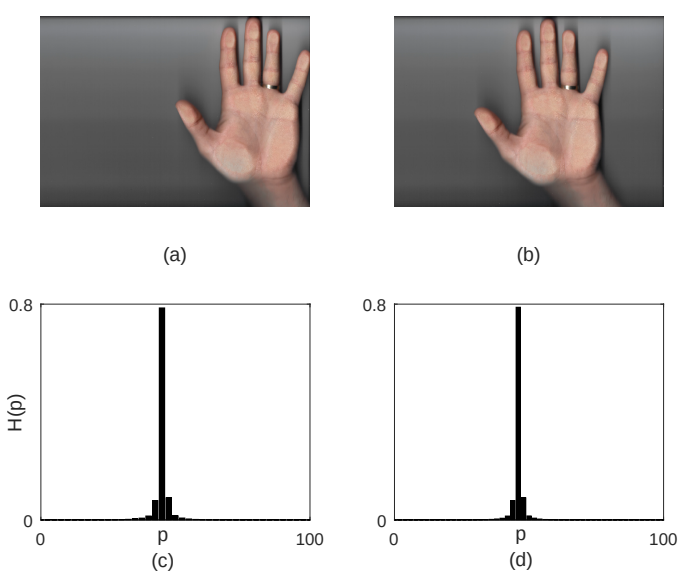

Figure 7. (a) a hand pattern; (b) shifted version of image in (a); (c) and (d) represent the normalized histograms of the HL sub band coefficients from images (a) and (b).

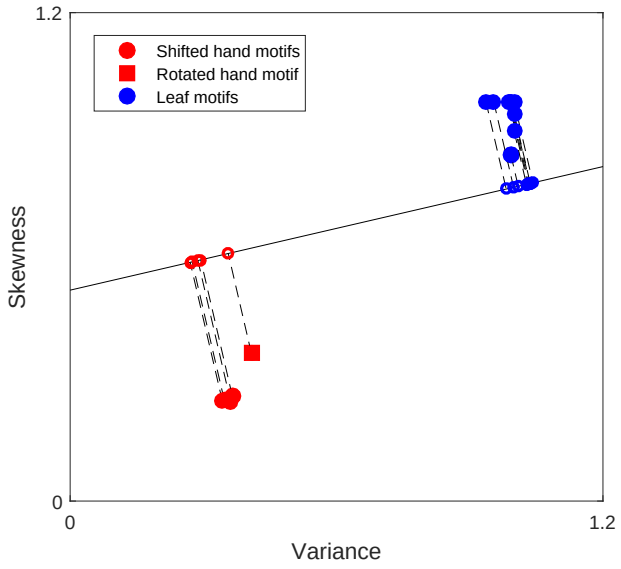

Figure 8. LDA projection of the two features from the hand and leaf image motifs; the distance between features within an image motif group is as minimum as possible and the distance between features of different image motif groups is large enough.

analysis (LDA) algorithm [1] [29].

LDA is a supervised method which projects the features from the samples of the two or more classes onto a lower dimensional space with good class separability in order to avoid over-fitting and computational costs reduction. This method provides a combination of features which separates the classes ideally with the minimum amount of error. The less the minimum error, the better is merit of the features. If the data can be separated linearly and correctly the error will be 0, and if the whole data cannot be classified linearly and correctly then the error has its maximum amount of 1. LDA finds the most discriminant projection by maximizing between-class distance and minimizing within-class distance. The experiments show that for most of the tested features the minimum error is between 0 and 0.01. Furthermore, the distance between feature clusters should be as great as possible to facilitate grouping.

Figure 8 demonstrates the result of the LDA projection of the two extracted features from the image motifs in Figure 5. It is obvious that the distance between the two groups is large enough in order to separate them correctly. Moreover, the distance between features belonging to the same image motif group (represented on the projection line) is minimized.

Since the 2D-CQTWP is shift-invariant, the first four hand images are as close as possible to each other and their projection on the projection line is at the same position. These images are depicted by the circle red marker. Nevertheless, the projection of the features extracted from the rotated image (illustrated by the square red marker) is not at the same position of other hand images. This illustrates that the 2D-CQTWP is not rotation invariant, however we are able to detect this image motif and separate it from other image motifs.

In the last step, the similarity between feature values is measured by Euclidean, Canberra and Dynamic Time Warping distance measures. Both Euclidean distance and Dynamic Time Warping performed similar in the case of small datasets (less than 50 images). These measures were able to detect 22 image motifs out of 25 inserted image motifs. The Canberra distance was able to discover 21 image motifs in the same data base.

Results of the stated similarity measures in Section III-C are depicted in Table. I. The presented results are obtained from the tested data set with 50 different inserted image motifs. Both Euclidean and DTW distance outperformed the Canberra distance. Euclidean and DTW distances detected the same amount of image motifs but, the image motifs were different. Since, the aforementioned image motif discovery approaches in Section II convert an image in a one dimensional signal, it is not possible to benchmark the performance of the proposed method against them.

TABLE I. Evaluating results of detected motifs, CR: Correct motif discovery rate, F-M: F-Measure, Sn: Sensitivity, Pr: Precision; ED: Euclidean distance, DTW: Dynamic Time Warping and CD: Canberra distance.

Similarity Measure	CR(%)	F-M(%)	Sn(%)	Pr(%)
ED	84.62	84.94	85.27	84.62
DTW	84.62	84.94	85.27	84.62
CD	83.85	84.82	85.83	83.85

V. Conclusion and Outlook

In this contribution, a method is presented to detect image motifs of various size. Detection of image motifs is performed within three steps: First, the Complex Quad Tree Wavelet Packet transform is applied to provide a comprehensive analysis of images in various frequency scales. This wavelet transform has efficient properties such as being shift-invariant. Moreover, its ability for analytic representation, is helpful in order to reduce aliasing.

 ISBN: 978-1-61208-549-4

The first four statistical moments and energy of the wavelet coefficients are extracted as feature values. Since motif discovery is an unsupervised task, there is no information about the tested images. Consequently, the statistical features are applied in this work, but depending on the task it is possible to employ other types of features.

In the next step, motifs are detected by measuring the similarity between their feature values. The performance of the proposed method is evaluated by different quality measures. One advantage of the proposed method is its ability to consider both images of fixed and variable lengths. In addition, as images are not transformed to a one dimensional representation form, no information is lost.

In the next approach, our aim will be to find the proper scale and nodes of the 2D-CQTWP with the best information content. Moreover, it is desirable to detect motifs within various images without segmenting them via a sliding window.

ACKNOWLEDGMENT

This research is partly supported by the International Graduate School of Intelligent Systems in Automation Technology (ISA), which is run by scientists of the Faculty of Computer Science, Electrical Engineering and Mathematics and the Faculty of Mechanical Engineering of the University of Paderborn and the Institute of Industrial Information Technologies (inIT) of the Ostwestfalen-Lippe University of Applied Sciences.

REFERENCES

[1] E. Alpaydın, Introduction to Machine Learning, 2nd ed. Cambridge: The MIT Press, 2010.

[2] S. A. Khan, M. Nazir, S. Akram, and N. Riaz, "Gender classification using image processing techniques: A survey," in 2011 IEEE 14th International Multitopic Conference. IEEE, 2011, pp. 25–30.

[3] S. S. Nath, G. Mishra, J. Kar, S. Chakraborty, and N. Dey, "A survey of image classification methods and techniques," in International Conference on Control, Instrumentation, Communication and Computational Technologies (ICCICCT). IEEE, 2014, pp. 554–557.

[4] S. Gangwar and R. P. Chauhan, "Survey of clustering techniques enhancing image segmentation process," in 2015 Second International Conference on Advances in Computing and Communication Engineering. IEEE, 2015, pp. 34–39.

[5] P. Esling and C. Agon, "Time-series data mining," vol. 45. ACM, 2012, pp. 1–34.

[6] M. K. Das and H.-K. Dai, "A survey of dna motif finding algorithms," BMC bioinformatics, vol. 8 Suppl 7, 2007, p. S21.

[7] P. Patel, E. Keogh, J. Lin, and S. Lonardi, "Mining motifs in massive time series databases," in Proceedings IEEE International Conference on Data Mining. IEEE, 2002, pp. 370–377.

[8] S. Torkamani and V. Lohweg, "Survey on time series motif discovery," in Journal: Wiley Interdisciplinary Reviews: Data Mining and Knowledge Discovery. Article ID: WIDM1199, 2017.

[9] X. Xi, E. Keogh, L. Wei, and A. Mafra-Neto, "Finding motifs in a database of shapes," in Proceedings of the 2007 SIAM international conference on data mining. SIAM, 2007, pp. 249–260.

[10] W. Hu, R. Hu, N. Xie, H. Ling, and S. Maybank, "Image classification using multiscale information fusion based on saliency driven nonlinear diffusion filtering," IEEE Transactions on Image Processing, vol. 23, no. 4, 2014, pp. 1513–1526.

[11] N. M. Zaitoun and M. J. Aqel, "Survey on image segmentation techniques," Procedia Computer Science, vol. 65, 2015, pp. 797–806, elsevier.

[12] K. Zhang, W. K. Leow, and Y. Cheng, Performance Analysis of Active Shape Reconstruction of Fractured, Incomplete Skulls. Springer International Publishing, 2015, pp. 312–324.

[13] B. K. Gayathri and P. Raajan, "A survey of breast cancer detection based on image segmentation techniques," in 2016 International Conference on Computing Technologies and Intelligent Data Engineering (ICCTIDE'16). IEEE, 2016, pp. 1–5.

[14] L. Ye and E. Keogh, "Time series shapelets: A new primitive for data mining," in Proceedings of the 15th ACM SIGKDD International Conference on Knowledge Discovery and Data Mining, ser. KDD '09. ACM, 2009, pp. 947–956.

[15] L. Chi, Y. Feng, H. Chi, and Y. Huang, "Face image recognition based on time series motif discovery," in IEEE International Conference on Granular Computing. IEEE, 2012, pp. 72–77.

[16] J. Grabocka, N. Schilling, M. Wistuba, and L. Schmidt-Thieme, "Learning time-series shapelets," in Proceedings of the 20th ACM SIGKDD International Conference on Knowledge Discovery and Data Mining, ser. KDD '14. ACM, 2014, pp. 392–401.

[17] T. Rakthanmanon, Q. Zhu, and E. Keogh, "Mining historical documents for near-duplicate figures," in IEEE 11th International Conference on Data Mining. IEEE, 2011, pp. 557–566.

[18] S. En, C. Petitjean, S. Nicolas, and L. Heutte, "Segmentation-free pattern spotting in historical document images," in 13th International Conference on Document Analysis and Recognition (ICDAR). IEEE, 2015, pp. 606–610.

[19] S. Torkamani, H. Dörksen, and V. Lohweg, "Multi-scale motif discovery in image processing," in Workshop on Probabilistic Graphical Models, Heidelberg, Germany, Oct 2015.

[20] I. W. Selesnick, R. G. Baraniuk, and N. G. Kingsbury, "The dual-tree complex wavelet transform," Signal Processing Magazine, IEEE, vol. 22, no. 6, 2005, pp. 123–151.

[21] S. Torkamani and V. Lohweg, "Shift-invariant feature extraction for time-series motif discovery," in 25. Workshop Computational Intelligence, ser. Schriftenreihe des Instituts für Angewandte Informatik - Automatisierungstechnik am Karlsruher Institut für Technologie, vol. 54. KIT Scientific Publishing, 2015, pp. 23–45.

[22] A. F. Abdelnour and I. W. Selesnick, "Symmetric nearly shift-invariant tight frame wavelets," IEEE Transactions on Signal Processing, vol. 53, no. 1, 2005, pp. 231–239, IEEE.

[23] C. S. Burrus, R. A. Gopinath, and H. Guo, Introduction to wavelets and wavelet transforms: A primer. Upper Saddle River and NJ: Prentice Hall, 1998.

[24] A. D. Polyanin and A. V. Manzhirov, Handbook of mathematics for engineers and sciencists. Boca Raton: Chapman & Hall/CRC, 2007.

[25] M. M. Deza and E. Deza, Encyclopedia of distances. Springer, 2009.

[26] M. B. Stegmann and D. D. Gomez, "A brief introduction to statistical shape analysis," 2002, informatics and Mathematical Modelling, Technical University of Denmark, DTU.

[27] P. F. B. Silva, A. R. S. Marcal, and da Silva R. A., "UCI machine learning repository: Leaf data set," 2014, last access: 06.04.17. [Online]. Available: https://archive.ics.uci.edu/ml/datasets/Leaf

[28] MathWorks, "MATLAB," 2017, last access: 06.04.17. [Online]. Available: https://de.mathworks.com/products/matlab.html

[29] C. Bayer, M. Bator, U. Mönks, A. Dicks, O. Enge-Rosenblatt, and V. Lohweg, "Sensorless drive diagnosis using automated feature extraction, significance ranking and reduction," in 18th IEEE Int. Conf. on Emerging Technologies and Factory Automation (ETFA 2013). IEEE, 2013, pp. 1–4.

 ISBN: 978-1-61208-549-4